Submitted for publication in the Astrophysical Journal Letters
Preprint typeset using LaTeX style emulateapj v. 5/2/11

STELLAR ACTIVITY AND EXCLUSION OF THE OUTER PLANET IN THE HD 99492 SYSTEM

Stephen R. Kane[1], Badrinath Thirumalachari[1], Gregory W. Henry[2], Natalie R. Hinkel[1,3], Eric L.N. Jensen[4], Tabetha S. Boyajian[5], Debra A. Fischer[5], Andrew W. Howard[6], Howard T. Isaacson[7], Jason T. Wright[8,9]

Submitted for publication in the Astrophysical Journal Letters

ABSTRACT

A historical problem for indirect exoplanet detection has been contending with the intrinsic variability of the host star. If the variability is periodic, it can easily mimic various exoplanet signatures, such as radial velocity variations that originate with the stellar surface rather than the presence of a planet. Here we present an update for the HD 99492 planetary system, using new radial velocity and photometric measurements from the Transit Ephemeris Refinement and Monitoring Survey (TERMS). Our extended time series and subsequent analyses of the Ca II H&K emission lines show that the host star has an activity cycle of ∼13 years. The activity cycle correlates with the purported orbital period of the outer planet, the signature of which is thus likely due to the host star activity. We further include a revised Keplerian orbital solution for the remaining planet, along with a new transit ephemeris. Our transit-search observations were inconclusive.

Subject headings: planetary systems – techniques: photometric – techniques: radial velocities – stars: individual (HD 99492)

1. INTRODUCTION

The radial velocity (RV) technique remains one of the most successful methods for the discovery of exoplanetary systems. At the present time, more than 500 exoplanets have been discovered using the RV technique, including a vast range of multi-planet systems and orbital configurations. The success of this method is greatly dependent upon the ability to accurately characterize the properties of the host star. In particular, the evolution of star spots, magnetic fields, and pulsations have well-studied effects on stellar radial velocity variations (Saar & Donahue 1997; Queloz et al. 2001; Desort et al. 2007; Hébrard et al. 2014). There have been numerous recent cases where stellar activity has posed a significant problem in the correct interpretation of RV data (Hatzes 2013; Hatzes et al. 2015; Robertson et al. 2014, 2015).

One source of activity-induced RV variations is that due to stellar activity cycles, analogous to the 11-year Solar cycle. Dravins (1985) predicted such a correlation, and Deming et al. (1987) reported the detection of such a correlation in the solar CO lines at 2.3μm, and inferred an amplitude of 30 m s^{-1} from the effect. Wright et al. (2008) argued that experience with the hundreds of sun-like stars from the California Planet Survey (CPS) showed that such effects are not so strong, and that activity cycles were probably not to blame for a ∼15 m s^{-1} RV variation in phase with an activity cycle in HD 154345. Similar high-amplitude RV-activity correlations in individual targets have been reported by Moutou et al. (2011), Carolo et al. (2014), and Robertson et al. (2013). Nonetheless, for most stars such correlations are small or absent, as argued by Wright et al. (2008) and Santos et al. (2010).

The star HD 99492 is an early-K dwarf in a binary orbit with HD 99491 (also known as 83 Leonis B and A, respectively). HD 99492 has a parallax of 55.7 ± 1.46 marcsec and a distance of 17.96±0.47 pcs (van Leeuwen 2007a,b). The mean angular separation of the stellar components is 40.76″, leading to an average projected separation of ∼730 AU. HD 99492 was found to harbor a 0.1 M_J planet in a 17 day orbit by Marcy et al. (2005). The best-fit Keplerian orbital solution at that time included a linear trend to account for a possible second companion in the system. The orbital elements were updated by Meschiari et al. (2011), who claimed to have resolved the separate orbit of an outer planet with a period of ∼5000 days.

Here we present new results for the system that reveal an activity cycle in the star and further show that stellar activity amply explains the signature of the outer planet (c). Section 2 provides new fundamental stellar parameters, including spectral analysis, discussion of element abundances, and activity indices from the complete dataset of 130 Keck/HIRES spectra. Section 3 presents our revised Keplerian orbital solution, including the correlation of the outer planet signature with the activity indices. Section 4 includes photometry from 5 observing seasons acquired over a span of 11 years. The photometric data confirms the absence of brightness variations in

skane@sfsu.edu
[1] Department of Physics & Astronomy, San Francisco State University, 1600 Holloway Avenue, San Francisco, CA 94132, USA
[2] Center of Excellence in Information Systems, Tennessee State University, 3500 John A. Merritt Blvd., Box 9501, Nashville, TN 37209, USA
[3] School of Earth & Space Exploration, Arizona State University, Tempe, AZ 85287, USA
[4] Dept of Physics & Astronomy, Swarthmore College, Swarthmore, PA 19081, USA
[5] Department of Astronomy, Yale University, New Haven, CT 06511, USA
[6] Institute for Astronomy, University of Hawaii, Honolulu, HI 96822, USA
[7] Astronomy Department, University of California, Berkeley, CA 94720, USA
[8] Department of Astronomy and Astrophysics, Pennsylvania State University, 525 Davey Laboratory, University Park, PA 16802, USA
[9] Center for Exoplanets & Habitable Worlds, Pennsylvania State University, 525 Davey Laboratory, University Park, PA 16802, USA

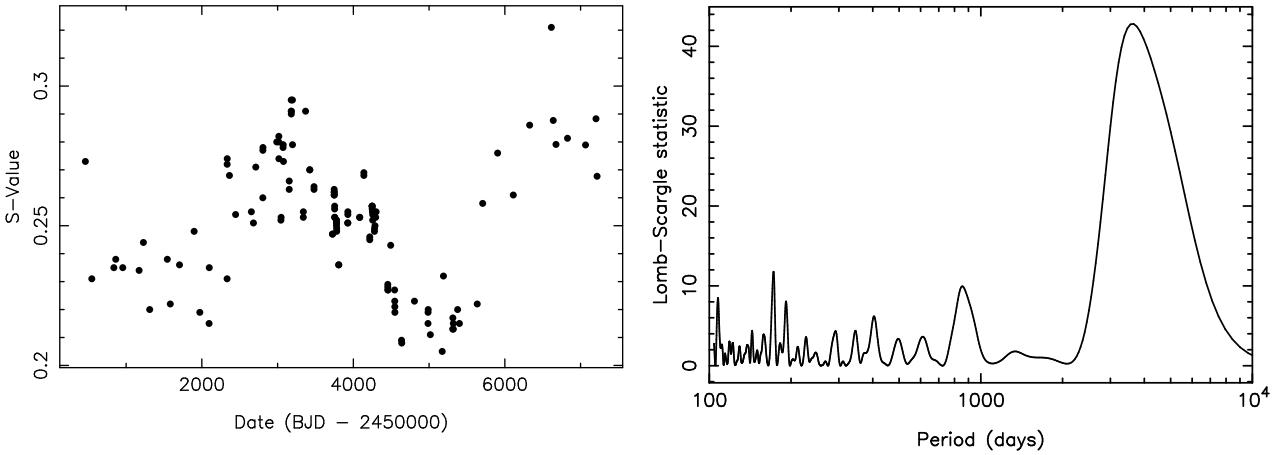

FIG. 1.— *Left*: HD 99492 S-values determined from the complete time series of Keck/HIRES spectra. *Right:* The periodogram resulting from a fourier analysis of the HD 99492 S-values, revealing a broad peak between 3000–5000 days.

phase with the orbital period of planet b, thus confirming the radial velocity variations in HD 99492 on a 17 day cycle are due to planetary reflex motion. Our limited number of brightness measurements near the predicted phase of planetary transit show no evidence for a transit but fall short of ruling them out. We provide concluding remarks in Section 5.

2. STELLAR PROPERTIES

2.1. *Fundamental Parameters*

The fundamental properties of HD 99492 have been previously determined, for example by Valenti & Fischer (2005); Takeda et al. (2007). We used an upgraded version of the Spectroscopy Made Easy (SME) package to model a Keck/HIRES spectrum of HD 99492. Details of the SME package may be found in Valenti & Piskunov (1996); Valenti & Fischer (2005). Briefly, SME uses an iterative technique that combines model atmosphere analysis with Yonsei-Yale model isochrones (Demarque et al. 2004) that utilize *Hipparcos* photometry and distances (van Leeuwen 2007a,b). This approach produces a self-consistent convergence with the measured surface gravity (Valenti et al. 2009).

The results of our analysis are shown in Table 1, including values for the surface gravity $\log g$, rotational velocity $v \sin i$, atmospheric abundance [Fe/H], effective temperature $T_{\rm eff}$ and stellar isochrone solution (mass $M_\star$, radius $R_\star$, and age). These parameters are consistent with previous estimates of the stellar properties and demonstrate that HD 99492 is a late-G/early-K dwarf with an age similar to the Sun.

2.2. *Stellar Abundances*

The element abundances of HD 99492 have been measured only by two groups to-date, namely Valenti & Fischer (2005) and Petigura & Marcy (2011). To correct for varying solar abundance normalizations, per the analysis within the Hypatia Catalog (Hinkel et al. 2014), each dataset was re-normalized to the Lodders et al. (2009) scale. The [Fe/H] measurement per both groups is 0.40 dex, since Petigura & Marcy (2011) adopted the stellar parameters and iron abundance from Valenti & Fischer (2005) in their analysis. From Petigura & Marcy (2011), [O/H] = 0.25 dex while Valenti & Fischer (2005) determined [Na/H] = 0.41, [Si/H] = 0.34 dex, [Ti/H] = 0.28 dex, and [Ni/H] = 0.38 dex. These results reveal a star that is markedly super-solar in both the volatile and refractory elements.

2.3. *Stellar Activity*

HD 99492 has been spectroscopically monitored using the HIRES echelle spectrometer (Vogt et al. 1994) on the 10.0m Keck I telescope as part of the CPS. For Keck/HIRES instrument configuration details, see Wright et al. (2004); Howard et al. (2009). Our complete HIRES dataset contains 130 measurements spanning over 18 years, extending the time baseline of the data reported by Meschiari et al. (2011) by over 5 years. The pipeline that extracts the RVs from the spectra (see Section 3) also extracts Ca II H&K line-profile variations and provides an index of stellar activity (Noyes et al. 1984). These data are calibrated to the Mt. Wilson S-values, defined as the ratio of the sum of the flux in the H&K line cores to the sum of the two continuum bands on either side (Wilson 1968). We include data acquired both before and after the upgrade of the HIRES CCD in 2004 August (Isaacson & Fischer 2010), taking into account the offset between pre-2004 and post-2004 calibrated datasets.

The time series of S-values are shown in the left panel of Figure 1. The periodic variation in S indicates that we have observed just over one complete cycle of stellar activity in the host star. To quantify the variation, we performed a fourier analysis of the time series, resulting in the periodogram shown in the right panel of Figure 1. This analysis reveals a broad peak in the power spectrum that lies between 3000–5000 days, with maximum power occurring at ∼3650 days. The S-value periodicity is thus consistent with the HD 99492c orbital period of 4970 ± 744 days determined by Meschiari et al. (2011). We elaborate further on the correlation between stellar activity and possible planetary signature in Section 3.

3. AN UPDATE TO THE PLANETARY SYSTEM

The RV measurements were extracted from the Keck/HIRES data with the use of an iodine cell mounted at the spectrometer entrance slit as a ro-

bust source of wavelength calibration (Marcy & Butler 1992; Valenti et al. 1995). The modeling procedure for the Doppler shift of each stellar spectrum with respect to the iodine spectrum is described further in Howard et al. (2009). The discovery orbital solution for the HD 99492 system by Marcy et al. (2005) included a linear trend component. The 93 RV measurements utilized by Meschiari et al. (2011) used a two-planet orbital solution to account for the previously-noted linear trend. A two-planet fit to our expanded dataset is able to recover a similar orbital solution to that previously found by Meschiari et al. (2011). Considering the periodic stellar activity described in Section 2.3 as a source for the previously observed linear trend and purported second planet, we performed a single-planet fit to our dataset of 130 RV measurements, both with and without a linear trend included. These fits were carried out using RVLIN, a partially-linearized, least-squares fitting procedure described in Wright & Howard (2009). The uncertainties in the resulting orbital parameters were estimated using the BOOTTRAN bootstrapping routines described in Wang et al. (2012). We included a stellar jitter noise component of 4 $\mathrm{m\,s^{-1}}$ in quadrature with the measurement uncertainties (Wright 2005; Butler et al. 2006). With our new dataset and its increased timespan, we find no evidence of a significant difference between the orbital fits that do and do not include a linear trend. We thus adopt the solution without the linear trend for which the complete orbital solution is shown in Table 1 and in the top panel of Figure 2. Note that the γ parameter shown in Table 1 is the systemic velocity of the system with respect to the zero point of the extracted RVs and thus is the systemic velocity relative to the template spectrum. The complete RV dataset of 130 measurements of HD 99492 are listed in Table 2.

To investigate further the impact of stellar activity on a two-planet solution (see Section 2.3), we compared the S-values with the RV residuals of the single-planet solution shown in Table 1. The resulting correlation diagram is shown in the bottom panel of Figure 2. We quantified the significance of the correlation using the Spearman rank correlation coefficient. The Spearman coefficient lies in the range $-1 < r_s < 1$, and, in turn, gives the probability that the two quantities being examined are not correlated. The Spearman coefficient for the data shown in the bottom panel of Figure 2 is $r_s = 0.39$, indicative of a positive correlation. The corresponding probability that the residuals of the single-planet solution and the S-values would produce the observed correlation if those quantities were in fact uncorrelated is 1.2×10^{-5}. We conducted a further test via an extensive Monte-Carlo simulation that performs a Fisher-Yates shuffle, randomizing the order of the residual data values. For each realization, the Spearman's rank correlation coefficient and probability were recalculated. This test resulted in a 0.5 probability of null-correlation, indicating that the correlation found above is robust. This implies, in turn, that the second planet claimed by Meschiari et al. (2011) is instead the result of stellar activity.

4. PHOTOMETRIC OBSERVATIONS

We observed HD 99492 photometrically as part of the Transit Ephemeris Refinement and Monitoring Survey (TERMS) (Kane et al. 2009) with the T12 0.8m Automatic Photoelectric Telescope (APT), one of several automated telescopes operated by Tennessee State University (TSU) at Fairborn Observatory in southern Arizona. The T12 APT is equipped with a precision, two-channel photometer that simultaneously measures the Strömgren b and y passbands using two EMI 9924QB photomultiplier tubes. This makes T12 ideal for achieving high photometric precision on relatively bright stars. The TSU APTs and their precision photometers, observing strategy, data reduction techniques, and photometric precision are described in detail by Henry (1999).

TABLE 1
System Parameters

Parameter	Value
HD99492	
V	7.58
$B-V$	1.0
Distance (pc)	55.7 ± 1.46
$T_{\rm eff}$ (K)	4929 ± 44
$\log g$	4.57 ± 0.06
$v \sin i$ ($\mathrm{km\,s^{-1}}$)	0.41 ± 0.5
[Fe/H] (dex)	0.3 ± 0.03
$M_\star$ ($M_\odot$)	0.85 ± 0.02
$R_\star$ ($R_\odot$)	0.78 ± 0.02
Age (Gyrs)	4.8 ± 4.1
HD 99492 b	
P (days)	17.054 ± 0.003
T_c [a] (JD – 2,440,000)	17367.776 ± 0.855
T_p [b] (JD – 2,440,000)	13776.317 ± 3.392
e	0.07 ± 0.06
ω (deg)	240.7 ± 75.4
K ($\mathrm{m\,s^{-1}}$)	6.98 ± 0.53
$M_p \sin i$ (M_J)	0.079 ± 0.006
a (AU)	0.123 ± 0.001
System Properties	
γ ($\mathrm{m\,s^{-1}}$)	-1.49 ± 0.37
Measurements and Model	
$N_{\rm obs}$	130
rms ($\mathrm{m\,s^{-1}}$)	4.33
$\chi^2_{\rm red}$	1.03

[a] Time of mid-transit.
[b] Time of periastron passage.

TABLE 2
HD 99492 Radial Velocities

Date (BJD – 2,440,000)	RV ($\mathrm{m\,s^{-1}}$)	σ ($\mathrm{m\,s^{-1}}$)
10462.113958	-3.09	1.49
10546.987859	-3.70	1.62
10837.932535	-3.30	1.56
10862.898993	-6.29	1.57
10955.876644	-8.27	1.21
11172.101597	-2.40	1.62
11228.035903	-8.13	1.51
11311.816319	2.63	1.59
11544.172650	-8.38	1.39
11582.974942	-0.25	1.35
11704.805914	-2.63	1.62
11898.154005	-15.85	1.48
11973.053090	4.30	1.39
12095.752049	-3.42	1.63
12097.753715	-8.23	1.56
12333.139410	5.37	1.69
12334.079884	7.42	1.73
12334.968322	2.05	1.53
12364.068125	2.33	1.46
12445.768264	-7.95	1.40

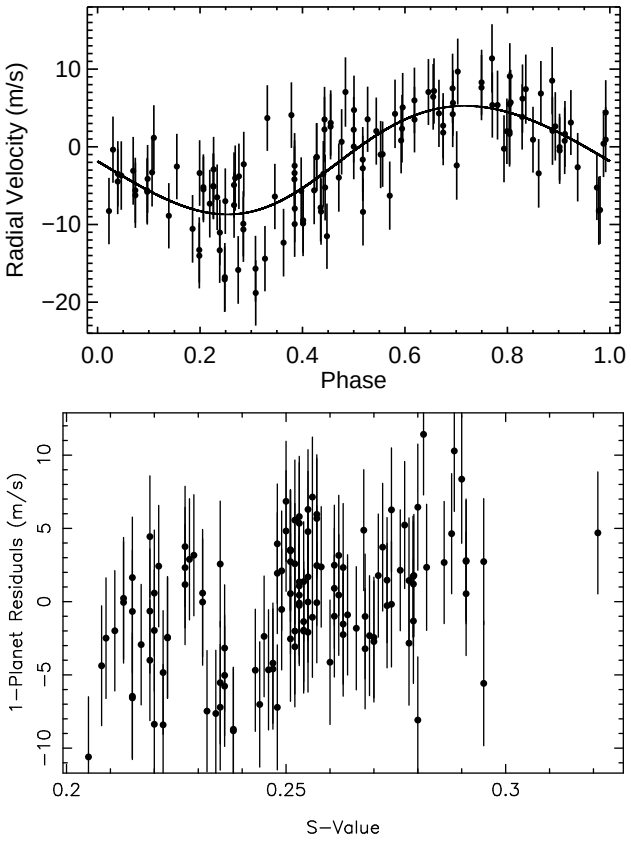

FIG. 2.— *Top*: The complete 130 RV measurement dataset phased on the best-fit Keplerian orbital solution for a single-planet system (see Table 1). *Bottom:* The residuals from the best-fit solution plotted against the activity indices described in Section 2.3. Our analysis shows that the probability of no correlation between the one-planet RV residuals and the S-values is 1.2×10^{-5}.

TABLE 2 — *Continued*

Date (BJD – 2,440,000)	RV ($m\,s^{-1}$)	σ ($m\,s^{-1}$)
12654.009595	5.07	1.70
12681.123484	-10.56	1.46
12711.858843	0.40	1.28
12804.765590	-7.83	1.43
12805.876296	4.73	1.68
12806.763634	-1.00	1.39
12989.171424	-16.78	1.60
13015.119444	11.38	1.59
13016.134363	6.20	1.59
13017.121921	8.51	1.38
13044.127569	-3.96	1.58
13045.999074	4.24	1.62
13071.870764	-4.13	1.51
13073.940752	-7.32	1.47
13076.983611	-5.70	1.42
13153.801470	-0.04	1.29
13153.804144	-0.48	1.28
13179.820787	-1.32	1.46
13179.824352	-1.33	1.57
13180.782037	7.05	1.78
13181.808171	2.02	1.35
13195.775914	-12.34	1.46
13196.794780	-5.61	1.47
13339.157731	5.37	0.89
13340.150718	3.85	0.95
13369.115093	3.54	0.92
13425.000741	1.95	0.97
13425.003310	1.67	1.02
13480.759734	-5.61	0.92
13480.761887	-6.24	0.90
13725.101748	-9.87	0.93

TABLE 2 — *Continued*

Date (BJD – 2,440,000)	RV ($m\,s^{-1}$)	σ ($m\,s^{-1}$)
13725.104595	-9.46	0.91
13747.133588	7.52	1.77
13747.138218	4.20	1.10
13747.145174	5.65	0.98
13748.096169	7.62	0.91
13748.098819	8.29	0.92
13753.040035	-4.47	0.91
13753.043380	-3.48	0.92
13754.021562	-5.64	0.92
13754.024097	-5.80	0.96
13775.980868	-3.38	0.96
13775.983125	-2.44	0.93
13776.976910	2.23	0.91
13776.979213	3.52	0.90
13777.950347	2.20	0.95
13777.952720	0.03	0.94
13779.971238	5.97	0.99
13779.974155	3.50	1.00
13806.916794	-13.28	0.95
13806.918981	-14.02	0.95
13926.762188	-5.05	0.99
13926.768762	-5.12	0.98
13927.761840	-9.91	0.90
13927.764213	-10.64	0.82
14084.153623	2.60	1.02
14084.157870	3.07	0.94
14139.063102	2.72	0.86
14139.064722	1.83	0.92
14216.896134	-13.32	0.91
14216.899722	-11.04	0.99
14246.798900	0.92	0.85
14246.800718	4.41	0.75
14248.811678	1.16	0.87
14250.800613	-2.91	0.84
14251.804815	-2.25	0.82
14255.765556	-1.65	0.89
14255.766991	-2.77	0.90
14277.743067	5.72	0.85
14278.749942	6.86	0.83
14279.748507	3.12	0.82
14285.751910	-3.80	0.97
14294.758669	5.47	0.97
14300.738970	-2.54	0.96
14455.109028	-5.20	1.04
14455.110868	-5.48	1.06
14456.129444	-4.92	0.96
14456.131400	-7.51	0.92
14493.134583	-8.34	1.17
14544.982280	0.64	0.95
14546.963137	0.81	1.03
14547.871944	7.05	1.10
14548.847407	9.68	1.10
14635.754444	2.00	0.98
14638.750949	-5.25	0.86
14807.164861	0.91	1.08
14985.837363	-14.40	0.93
14986.825959	-9.95	1.00
14987.839171	-5.24	1.08
15016.744103	-8.88	0.93
15173.123927	-18.81	0.94
15190.171113	-15.69	1.05
15311.807895	-3.49	1.09
15313.781452	-0.95	0.97
15319.842967	0.77	1.23
15319.850617	1.65	1.11
15376.739902	-17.07	0.89
15400.735697	6.43	1.01
15635.955861	-11.51	0.94
15707.736240	7.18	0.95
15905.166211	-6.50	1.01
16111.736847	-6.40	0.95
16328.051766	-0.37	1.17
16614.127514	9.08	1.15
16639.094368	-4.03	0.91
16675.173277	-4.19	1.18
16827.757817	3.70	1.03

TABLE 2 — *Continued*

Date (BJD – 2,440,000)	RV ($m\,s^{-1}$)	σ ($m\,s^{-1}$)
17065.116057	-7.00	1.02
17203.750309	4.08	1.01
17217.748571	-3.38	1.02

The T12 telescope acquired 368 nightly observations of HD 99492 during the 2004, 2009, 2010, 2013, and 2014 observing seasons. These data are plotted against Heliocentirc Julian Date in the top panel of Figure 3. The observations are insufficient to detect the long-term activity cycle described in Section 2.3. Therefore, we removed very small season-to-season variability in HD 99492 and/or its comparison stars by normalizing the final four observing seasons so their means match the first season, indicated by the horizonal dotted line in the top panel. This removal of seasonal variability allows a more sensitive search for variability that might be due to rotational modulation of star spots (e.g., Henry et al. 2013). Marcy et al. (2005) estimated the rotation period of HD 99492 to be around 45 days from the Ca II H and K emission strength. Our nightly observations scatter about the mean with a standard deviation 0.00484 mag, somewhat more than the typical measurement precision. However, Fourier analyses of the complete normalized data set and the individual observing seasons did not reveal any significant periodicities between 1 and 100 days that might correspond to the star's rotation period.

We further examined publicly available photometric data from the *Hipparcos* satellite to search for evidence of periodicity in the lightcurve of HD 99492 (Perryman et al. 1997; van Leeuwen 2007a). The data were extracted from the NASA Exoplanet Archive (Akeson et al. 2013), including 71 measurements spanning a period of 1,062 days and with a standard deviation of 0.135 mag. Our fourier analysis of the *Hipparcos* did not reveal strong periodicity, with the possible exception of a minor fourier power at ∼15.8 days.

The Keplerian orbital solution in Section 3 includes an estimate of T_c, the predicted time of mid-transit should the planetary orbital inclination be suitably close to edge-on. To determine the remainder of the predicted transit parameters, we adopted the SME stellar radius from Table 1 and an estimated planetary radius of $R_p = 0.52\ R_J$ using the mass-radius relationship described by Kane & Gelino (2012). Taking into account the orbital eccentricity from the Keplerian orbit (Kane & von Braun 2008), the transit probability is 2.8% and the predicted duration and depth for a central transit are 0.181 days and 0.54% respectively.

The APT observations are replotted in the middle panel of Figure 3. These data are phased with the orbital period and the predicted transit time shown in Table 1. We use least-squares to fit a sine curve to the data, also phased on the 17.054-day orbital period. This yields a formal semi-amplitude of the sine curve of just 0.00041 ± 0.000033 mag. The relatively small amplitude confirms that the observed RV variations are due to the presence of a planet rather than intrinsic stellar brightness variations.

The APT observations within ±0.06 phase units of the predicted transit time are shown in the bottom panel of Figure 3. The solid curve for the predicted transit signature includes the predicted mid-transit at phase 0.0, the transit depth (0.5%), and transit duration (±0.005 phase units). The vertical dashed lines represent the uncertainty in our new time of transit. We find no evidence for transits although our data do not rule them out completely. Monitoring observations were made on the night of 31 January 2016 UT, during a predicted transit, with the T12 APT and with the 0.6m telescope at Swarthmore's Peter van de Kamp Observatory. The night was marginally photometric at both sites; again, no evidence for transits was seen but we are still not able to completely rule them out.

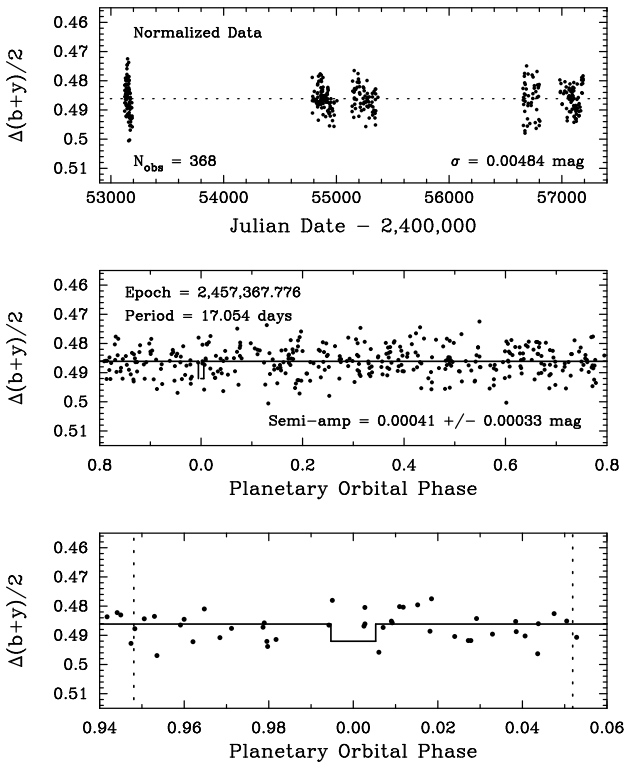

FIG. 3.— *Top*: Nightly photometric observations of HD 99492 from the 2004, 2009, 2010, 2013, and 2014 observing seasons acquired with the T12 0.8 m APT. The final four seasons have been normalized so their seasonal means match the 2004 season. *Middle*: The APT observations phased with the orbital period of 17.054 days. A sine fit to the phased observations yields a semi-amplitude of 0.00041 ± 0.00033 mag. This is consistent with the absense of light variability on the radial velocity period and also consistent with planetary reflex motion of the star as the cause of the RV variations. *Bottom*: The APT observations within ±0.06 phase units of the predicted transit time. The solid curve for the predicted transit shows the predicted mid-transit at phase 0.0, the transit depth (0.5%), and the duration (±0.005 phase units) for a central transit of planet b. The vertical dashed lines represent the uncertainty in the time of transit. Our photometry shows no evidence for transits but cannot rule them out completely.

5. CONCLUSIONS

The presence of stellar activity presents continuing challenges to exoplanet detection and characterization. Radial velocity exoplanet survey targets are usually chosen for their low chromospheric activity, leading to a bias against activity in the sample of bright planet-host stars. HD 99491 is an evolved star and has been known to exhibit chromospheric activity for some time (Zarro 1983; Wright et al. 2004). It is thus quite interesting to

find that the companion star, HD 99492, exhibits similar behavior over long timescales. It is hoped that continued photometric monitoring will help to resolve the complete magentic cycle of the star, such as those found for HD 192263 (Dragomir et al. 2012), although the target is very difficult to observe due to the small angular separation of the binary components.

The update to the parameters for the HD 99492 system presented here refines the stellar and planetary orbital parameters for the system. The update shows that the ∼5000 day RV signal is due to stellar activity rather than a planet. However, there are likely other planets of smaller mass and/or larger separation that lie beneath the current noise floor. As the exploration of exoplanetary systems forges onward to ever smaller planets, the careful examination of stellar activity is becoming more relevant than ever before.

ACKNOWLEDGEMENTS

GWH acknowledges long-term support from Tennessee State University and the State of Tennessee through its Centers of Excellence program. This research has made use of the NASA Exoplanet Archive, which is operated by the California Institute of Technology, under contract with the National Aeronautics and Space Administration under the Exoplanet Exploration Program. The results reported herein benefited from collaborations and/or information exchange within NASA's Nexus for Exoplanet System Science (NExSS) research coordination network sponsored by NASA's Science Mission Directorate. The data presented herein were obtained at the W.M. Keck Observatory, which is operated as a scientific partnership among the California Institute of Technology, the University of California and the National Aeronautics and Space Administration. The Observatory was made possible by the generous financial support of the W.M. Keck Foundation. The authors wish to recognize and acknowledge the very significant cultural role and reverence that the summit of Mauna Kea has always had within the indigenous Hawaiian community. We are most fortunate to have the opportunity to conduct observations from this mountain.

REFERENCES

Akeson, R.L., Chen, X., Ciardi, D., et al. 2013, PASP, 125, 989
Butler, R.P., Wright, J.T., Marcy, G.W., et al. 2006, ApJ, 646, 505
Carolo, E., Desidera, S., Gratton, R., et al. 2014, A&A, 567, A48
Demarque, P., Woo, J.-H., Kim, Y.-C., Yi, S.K. 2004, ApJS, 155, 667
Deming, D., Espenak, F., Jennings, D.E., Brault, J.W., Wagner, J. 1987, ApJ, 316, 771
Desort, M., Lagrange, A.-M., Galland, F., Udry, S., Mayor, M. 2007, A&A, 473, 983
Dragomir, D., Kane, S.R., Henry, G.W., et al. 2012, ApJ, 754, 37
Dravins, D. 1985, in Stellar Radial Velocities, Proceedings of IAU Colloquium No. 88, ed. A.G.D. Philip & D.W. Latham, 311-320
Hatzes, A.P. 2013, ApJ, 770, 133
Hatzes, A.P., Cochran, W.D., Endl, M., et al. 2015, A&A, 580, 31
Hébrard, É.M., Donati, J.-F., Delfosse, X., Morin, J., Boisse, I., Moutou, C., Hébrard, G. 2014, MNRAS, 443, 2599
Henry, G.W. 1999, PASP, 111, 845
Henry, G.W., Kane, S.R., Wang, S.X., et al. 2013, ApJ, 768, 155
Hinkel, N.R., Timmes, F.X., Young, P.A., Pagano, M.D., Turnbull, M.C. 2014, AJ, 148, 54
Howard, A. W., Johnson, J.A., Marcy, G.W., et al. 2009, ApJ, 696, 75
Isaacson, H., Fischer, D. 2010, ApJ, 725, 875
Kane, S.R., von Braun, K. 2008, ApJ, 689, 492
Kane, S.R., Mahadevan, S., von Braun, K., Laughlin, G., Ciardi, D.R. 2009, PASP, 121, 1386
Kane, S.R., Gelino, D.M. 2012, PASP, 124, 323
Lodders, K., Plame, H., Gail, H.-P. 2009, Landolt-Börnstein - Group VI Astronomy and Astrophysics Numerical Data and Functional Relationships in Science and Technology Volume 4B: Solar System. Edited by J.E. Trümper, 4B, 44
Marcy, G.W., Butler, R.P. 1992, PASP, 104, 270
Marcy, G.W., Butler, R.P., Vogt, S.S., et al. 2005, ApJ, 619, 570
Meschiari, S., Laughlin, G., Vogt, S.S., et al. 2011, ApJ, 727, 117
Moutou, C., Mayor, M., Lo Curto, G., et al. 2011, A&A, 527, A63
Noyes, R.W., Hartmann, L.W., Baliunas, S.L., Duncan, D.K., Vaughan, A.H. 1984, ApJ, 279, 763
Perryman, M.A.C., Lindegren, L., Kovalevsky, J., et al. 1997, A&A, 323, L49
Petigura, E.A., Marcy, G.W. 2011, ApJ, 735, 41
Queloz, D., Henry, G.W., Sivan, J.P., et al. 2001, A&A, 379, 279
Robertson, P., Endl, M., Cochran, W.D., MacQueen, P.J., Boss, A.P. 2013, ApJ, 774, 147
Robertson, P., Mahadevan, S., Endl, M., Roy, A. 2014, Science, 345, 440
Robertson, P., Roy, A., Mahadevan, S. 2015, ApJ, 805, L22
Saar, S.H., Donahue, R.A. 1997, ApJ, 485, 319
Santos, N.C., Gomes da Silva, J., Lovis, C., Melo, C. 2010, A&A, 511, A54
Takeda, G., Ford, E.B., Sills, A., et al. 2007, ApJS, 168, 297
Valenti, J.A., Butler, R.P., Marcy, G.W. 1995, PASP, 107, 966
Valenti, J.A., Piskunov, N. 1996, A&AS, 118, 595
Valenti, J.A., Fischer, D.A. 2005, ApJS, 159, 141
Valenti, J.A., Fischer, D., Marcy, G.W., et al. 2009, ApJ, 702, 989
van Leeuwen, F. 2007a, Hipparcos, the New Reduction of the Raw Data, Astrophys. Space Sci. Lib., 350
van Leeuwen, F. 2007b, A&A, 474, 653
Vogt, S.S., Allen, S.L., Bigelow, B.C., et al. 1994, Proc. SPIE, 2198, 362
Wang, S.X., Wright, J.T., Cochran, W., et al. 2012, ApJ, 761, 46
Wilson, O.C. 1968, ApJ, 153, 221
Wright, J.T., Marcy, G.W., Butler, R.P., Vogt, S.S. 2004, ApJS, 152, 261
Wright, J.T. 2005, PASP, 117, 657
Wright, J.T., Marcy, G.W., Butler, R.P., et al. 2008, ApJ, 683, L63
Wright, J.T., Howard, A.W. 2009, ApJS, 182, 205
Zarro, D.M. 1983, ApJ, 267, L61